



Natural dyes extracted from *Ligustrum vulgare*, *Juniperus sabina*, and *Papaver rhoeas* for novel DSSC applications

Makbule Erdoğan^{a,*}, Abdullah Atilgan^b, Yusuf Erdoğan^c, Abdullah Yildiz^b

^a Department of Landscape Architects, Faculty of Agriculture, Kırşehir Ahi Evran University, Kırşehir 40100, Türkiye

^b Department of Energy Systems Engineering, Faculty of Engineering and Natural Sciences, Ankara Yıldırım Beyazıt University, Ankara 06010, Türkiye

^c Department of Physics, Faculty of Science, Gazi University, Teknikokullar, Ankara 06500, Türkiye

ARTICLE INFO

Keywords:

Solar energy materials
Spectroscopy
FTIR
Energy storage and conversion

ABSTRACT

An effective extraction strategy has been devised to get natural dye sensitizers from *Ligustrum vulgare* fruit (M1), *Juniperus sabina* fruit (M6), and *Papaver rhoeas* petal (M9) to produce dye-sensitized solar cells (DSSCs). The power conversion efficiencies (PCE) achieved from the DSSCs with dyes extracted from *Ligustrum vulgare* fruit, *Juniperus sabina* fruit, and *Papaver rhoeas* petal are 0.48 %, 0.55 %, and 0.42 %, respectively. The improved photovoltaic efficiency of the DSSCs created using *Juniperus sabina* fruit can be primarily due to the notable increase in the open circuit voltage, which reached 0.66 V.

1. Introduction

Applying natural dyes in DSSCs is a significant utilization of these dyes, showcasing their broad functionality. DSSCs use a photosensitive sensitizer to capture solar radiation and efficiently convert it into electrical energy. Therefore, using dyes as sensitizers is a critical element in the functioning of DSSCs. There are synthetic dyes specially designed for this specific purpose. Natural dyes are an alternative to synthetic dyes due to their cost efficiency, environmental friendliness, and abundant availability. Researchers are working to improve the effectiveness of DSSC by utilizing natural dyes [1–3].

The present study focused on the production of DSSC utilizing natural dyes extracted from *Ligustrum vulgare* fruit, *Juniperus sabina* fruit, and *Papaver rhoeas* petal. Based on our current knowledge, this study is the first investigation into the photovoltaic capabilities of DSSC derived from natural dyes. This research study aims to investigate the impact of dyes on photovoltaic performance to gain a more comprehensive understanding of their properties.

2. Plant material and preparation of natural dye

The information about the taxonomic classification of *Ligustrum vulgare*, *Juniperus sabina*, and *Papaver rhoeas* is given in the [supplementary material](#). The botanical specimens, *Ligustrum vulgare* fruits, *Juniperus sabina* fruits, and *Papaver rhoeas* petals, were obtained from the

Kırşehir region in Turkey (Fig. 1a). The voucher specimen was deposited at the herbarium of Kırşehir Ahi Evran University. The fruits and petals were dried at 50 °C for 24 h. Following this, the dried samples were ground into a fine powder. The extraction process involved using 50 mL of methanol for *Ligustrum vulgare* fruit and 50 mL of 96 % ethanol for *Juniperus sabina* fruits and *Papaver rhoeas* petals, with a mass of 2 gr. The extraction procedure was conducted on a per-sample basis, with each sample being heated at a temperature of 40 °C using a mixer for 24 h. The extract-filtrated samples were kept at +4 °C and protected from exposure to light (Fig. 1b).

3. Results and discussion

3.1. UV–Vis and FT-IR spectroscopy of natural dyes

The presence of anthocyanin and flavonoid compounds is of utmost importance in facilitating the transfer of electrons from excited dye molecules to TiO₂. The M1 dye obtained from the methanolic extract of *Ligustrum vulgare* fruit contains anthocyanins and flavonoids [4]. Amentoflavone has been identified as the main component of the ethanolic extract derived from the fruit of *Juniperus sabina* for the M6 dye solution [5]. Anthocyanins are the primary chemical constituents of the ethanolic extract of M9 dye from *Papaver rhoeas* petals [6,7].

The [supplementary material](#) provides details regarding the FT-IR and UV–Vis spectra. The capacity of anthocyanin and flavonoid compounds

* Corresponding author.

E-mail address: merdogdu@ahievran.edu.tr (M. Erdoğan).

to engage with TiO_2 is attributed to the presence of carbonyl and hydroxyl groups [8], which promote the electron transfer mechanism. The spectral range of $3100\text{--}3500\text{ cm}^{-1}$ [9] displayed a prominent peak attributed to the vibrational modes of the hydroxyl group. The FT-IR spectra (Fig. 1c) of the M1, M6, and M9 dyes have peaks at 3363 cm^{-1} , 3617 cm^{-1} , and 3586 cm^{-1} , respectively, which suggest the presence of the O-H functional group. The peak detected at around 1720 cm^{-1} [9] can be attributed to the stretching vibration mode of the carbonyl functional group. The presence of the carbonyl functional group can be detected in the FT-IR spectra of the M9, M6, and M1 dyes, with characteristic wavenumbers of 1718 cm^{-1} , 1693 cm^{-1} , and 1702 cm^{-1} , respectively.

Fig. 1d displays the UV-Vis absorption spectra of the dye extraction solutions. The peak absorbance of the M9 dye is observed at a wavelength of 577 nm , indicating that the spectral absorption range for the anthocyanin region is from $450\text{ to }600\text{ nm}$. Anthocyanins play a significant role in the pigmentation of poppy petals, resulting in their red color [10]. It can be noted that the absorbance of M1 is significantly lower when compared to that of M9. The wavelength at which the M1 exhibits maximum absorbance is determined to be 533 nm . M6 containing chlorophyll appears at a spectral peak at a wavelength of 670 nm .

3.2. Photovoltaic characterization

The information about the fabrication of DSSC devices is given in the supplementary material. Table 1 displays the photovoltaic parameters of the devices, encompassing the open-circuit voltage (V_{oc}), short-circuit current density (J_{sc}), fill factor (FF), and photovoltaic efficiency (η). Fig. 2a depicts the current density-voltage curves of the DSSC fabricated using the dyes mentioned above. The M6 dye-based DSSC exhibits a superior maximum PCE of 0.55% compared to the efficiencies achieved

by M1 and M9 dyes. These values can be attributable to the solar cell J_{sc} value of 1.02 mA/cm^2 , V_{oc} value of 0.66 V , and FF of 82% . Notably, the DSSC, specifically those incorporating M9, demonstrated a greater J_{sc} of 1.22 mA/cm^2 than the DSSC using M1 and M6.

Nevertheless, the V_{oc} exhibited by the DSSC utilizing M9 was significantly diminished, resulting in a decreased overall efficiency compared to the DSSC using M6. The occurrence of charge recombination in the device can be attributed to the reduction in V_{oc} reported in DSSCs employing M9 dye. After the M1 dye is applied onto the surface of TiO_2 , there is an increase in the V_{oc} from 0.56 V (for M9) to 0.64 V . Furthermore, it should be noted that the FF exceeds that of M6 and M9, with a value of 0.88 . However, it is worth mentioning that the J_{sc} shows a drop, reaching 0.85 mA/cm^2 . As a result, the application of M1 led to a notable decrease in efficiency, measuring at 0.48% . The comparable photocurrent seen in devices based on M6 and M9 can be explained by considering the balance between the quantity of dye deposited on TiO_2 and the UV-visible spectrum response. It can be deduced that anodes containing M6 demonstrate the most significant potential for success compared to alternative dyes utilized in DSSC applications.

An in-depth examination of the interfacial characteristics of devices employing M1, M6, and M9 dyes was conducted using electrochemical impedance spectroscopy (EIS). The assessment covered a range of frequencies from 1 MHz to 1 Hz , with a bias voltage that roughly approximated the V_{oc} . Table 1 provides a concise overview of the characteristics of the elements identified through the utilization of an appropriate equivalent circuit.

Fig. 2b presents the Nyquist graphs mentioned in a prior paper [11]. R_{CT} , R_{REC} , and R_s information are described in detail in the Supplementary material. The randomized controlled trial (R_{CT}) prefers the M6 M9 M1 sequence. Regarding M1, a correlation exists between the observed changes in R_{CT} and the fluctuations reported in the J_{sc} values of DSSC employing M6 and M9 dyes. This suggests that the variable

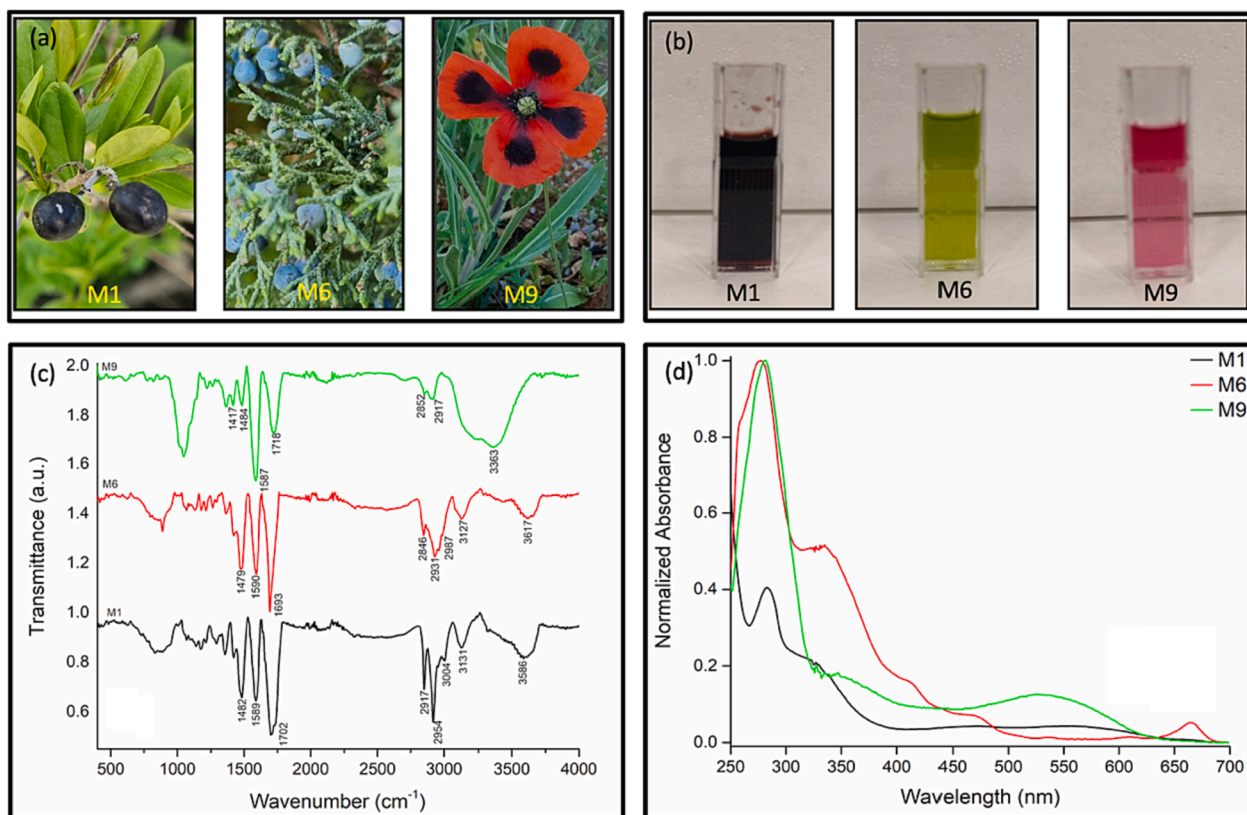


Fig. 1. A) *Ligustrum vulgare* fruits (M1), *Juniperus sabina* fruits (M6), and *Papaver rhoeas* petals (M9), b) the dye solutions, c) FT-IR, and d) UV-Vis spectra of the dye solutions.

Table 1
Photovoltaic performance (a), the parameters derived from EIS measurements (b) of the devices.

Dye	J_{SC} (mA/cm ²)	V_{OC} (mV)	FF	η (%)	R_s (W)	R_{ct} (W)	R_{rec} (W)	η_c (%)
M1	0.85±0.16	0.64±0.039	0.88±0.08	0.48±0.049	41.07	11.91	182.2	93.86
M6	1.02±0.14	0.66±0.042	0.82±0.07	0.55±0.041	41.86	3.82	272.3	98.62
M9	1.22±0.11	0.56±0.021	0.62±0.05	0.42±0.011	41.22	5.99	142.1	95.95

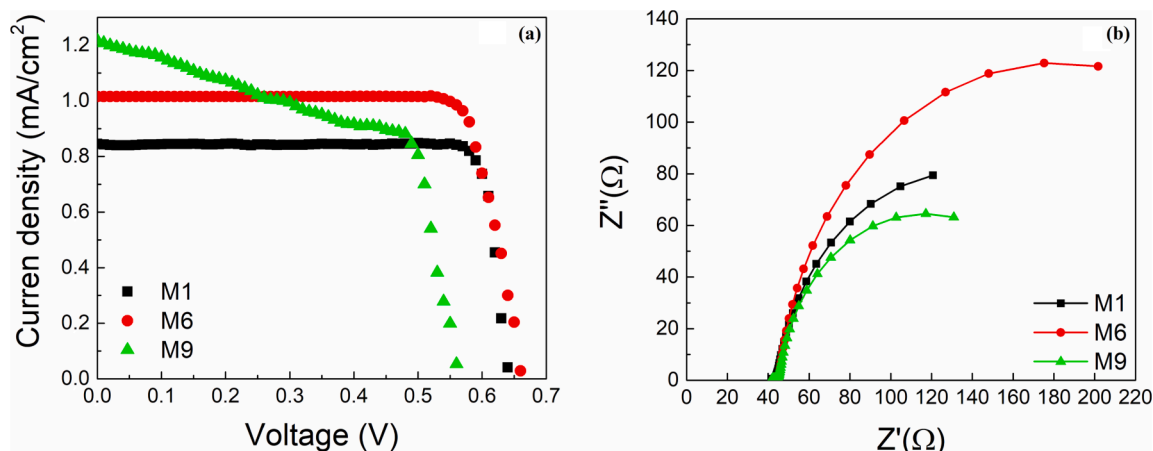


Fig. 2. The J-V characteristics (a) and EIS measurements (b) of the devices.

under investigation, R_{CT} , had a noticeable impact on the observed variations in J_{SC} measurements. Based on the calculated value of R_{REC} obtained from Fig. 2b, the recombination rate at the interface of the photoanode is somewhat lower for devices utilizing M6 compared to those utilizing M1 and M9. Additionally, it was noted that the device utilizing M6 demonstrated the highest R_{REC} value, indicating that the M6-based device possesses a superior V_{OC} compared to its counterparts and boosts the overall efficiency of the device. The determination of the charge collecting efficiency (η_c) for the devices can be obtained by utilizing the measured impedance data and applying the equation $\eta_c = [1 + (R_{ct}/R_{rec})]^{-1}$ [12]. The data demonstrates a sequential pattern in the following sequence: The device based on M6 demonstrates enhanced performance in charge transfer and recombination suppression compared to other dyes, as seen by the hierarchy $M1 < M9 < M6$. The patterns detected in the values of R_{CT} demonstrate a notable level of resemblance. This factor may act as an additional element contributing to the improved PCE of M6-based devices compared to devices that employ alternative dyes.

Table 2 compares the DSSCs investigated in the current research and other DSSCs documented utilizing natural dyes. The new dye exhibits superior characteristics in comparison to alternative dyes. Identifying an enhanced photo-to-electric conversion efficiency implies a notable association between the dye molecules and TiO_2 , demonstrating a robust connection between these entities.

4. Conclusions

In brief, our research employed novel natural dye sensitizers obtained from *Ligustrum vulgare*, *Juniperus sabina*, and *Papaver rhoeas* to fabricate DSSCs. This represents the initial documented case of utilizing these sensitizers in the literature. The dye sensitizers examined in this study have positive characteristics that make them promising candidates for use as cost-effective dyes in DSSCs. The sensitizers under consideration exhibit certain advantages in comparison to their natural dye counterparts, specifically in terms of cost-effectiveness and performance. As a result, the device comprising a *Juniperus sabina* photoanode demonstrated the best efficiency, measuring 0.55 %.

Table 2
Comparison of the results for various DSSCs based on natural dyes.

Source	J_{SC} (mA/cm ²)	V_{OC} (V)	FF	η (%)	Reference
Rosella	1.63	0.41	0.57	0.37	[13]
C. Fistula flower	0.54	0.51	0.65	0.21	[14]
Spinach	0.41	0.59	0.58	0.17	[15]
Nasturtium	0.72	0.55	0.70	0.28	[16]
Ipomoea	0.91	0.54	0.56	0.28	[17]
Cosmos sulphureus	1.04	0.45	0.61	0.54	[18]
Juniperus sabina	1.02	0.66	0.82	0.55	This study

CRedit authorship contribution statement

Makbule Erdoğan: Conceptualization, Data curation, Funding acquisition, Investigation, Methodology, Writing – original draft, Writing – review & editing. **Abdullah Atılgan:** Data curation, Formal analysis, Visualization. **Yusuf Erdoğan:** Conceptualization, Investigation, Resources, Writing – original draft, Writing – review & editing. **Abdullah Yıldız:** .

Declaration of competing interest

The authors declare that they have no known competing financial interests or personal relationships that could have appeared to influence the work reported in this paper.

Data availability

Data will be made available on request.

Acknowledgment

The authors thank Dr. Ufuk ÖZBEK for his assistance in scientifically identifying the plant.

Appendix A. Supplementary data

Supplementary data to this article can be found online at <https://doi.org/10.1016/j.matlet.2024.135811>.

[org/10.1016/j.matlet.2023.135811](https://doi.org/10.1016/j.matlet.2023.135811).

References

- [1] M. Erdoğan, et al., *Journal of Photochemistry and Photobiology a: Chemistry* 448 (2024) 115288.
- [2] N. Sarwar, et al., *Solar Energy* 257 (2023) 314–323.
- [3] A.S. Teja, et al., *Dyes and Pigments* 210 (2023) 110997.
- [4] I. Alouani, et al., *Int J Pharm Pharm Sci.* 8 (10) (2016) 21.
- [5] N. Orhan, et al., *Iranian Journal of Pharmaceutical Research* 16 (2017) 64.
- [6] G. Matysik, et al., *Chromatographia* 32 (1991) 19–22.
- [7] D.A. Kostic, et al., *Journal of Medicinal Plants Research* 4 (17) (2010) 1727–1732.
- [8] R. Ramamoorthy, et al., *Journal of Applied Electrochemistry* 46 (2016) 929–941.
- [9] Y. Erdoğan, et al., *Journal of Molecular Structure* 1221 (2020) 128873.
- [10] P. Schauenberg, F., et al., *Paris Guide des plantes médicinales*, Delachau et Niestlé, Paris, 1977.
- [11] N. Akdogan, et al., *Materials Letters* 351 (2023) 135075.
- [12] S. Shogh, et al., *Materials Letters* 159 (2015) 273–275.
- [13] K. Wongcharee, et al., *Solar Energy Materials and Solar Cells* 91 (7) (2007) 566–571.
- [14] A.K. Rajan, et al., *Journal of Nanophotonics* 13 (3) (2019) 036007.
- [15] A.M. Ammar, et al., *Journal of Nanomaterials* (2019) 1867271.
- [16] S. Singh, et al., *Optik* 243 (2021) 167331.
- [17] H. Chang, et al., *Journal of Alloys and Compounds* 495 (2) (2010) 606–610.
- [18] M. Narayan, et al., *Applied Solar Energy* 47 (2011) 112–117.